Polymer Bulletin (2023) 80:12835–12848
https://doi.org/10.1007/s00289-023-04670-3

ORIGINAL PAPER

Synthesis, crystal structure and dielectric properties of a hybrid dihydrogen arsenate salt: $(C_9H_{11}N_4)H_2AsO_4$

Omar Kammoun[1,2] · Mohamed Abdelhedi[3] · Mohamed Boujelbene[1]

Received: 14 October 2022 / Revised: 26 December 2022 / Accepted: 30 December 2022 /
Published online: 16 January 2023

Abstract

The use of the organic aromatic amine molecule 5-amino-3-methyl-1-phenyl-1H-1,2,4-triazole to synthesize a dihydrogen arsenate hybrid salt leads to a supramolecular structure type. Single crystals of $(C_9H_{11}N_4)H_2AsO_4$ were grown through slow evaporation in solution. The synthesized compound crystallizes in the monoclinic system with the non-centrosymmetric $P2_1$ space group according to the following parameters; $a=9.655$ (3) Å, $b=4.7090$ (15) Å, $c=14.022$ (4) Å, $\beta=108.147$ (5)° and $Z=4$. The mineral part building from dihydrogen arsenate anions $[H_2AsO_4]^-$ is linked together and to the organic cations $[C_9H_{11}N_4]^+$ by hydrogen bonds only. The results of Hirshfeld's analysis show that in all possible molecular contacts, the hydrogen–hydrogen and the oxygen–hydrogen are the most important interaction in the crystal (37.5 and 31.9%, respectively). The Fourier transform infrared (FT-IR) confirms the existence of vibrational modes corresponding to the organic amine molecule and mineral arsenate tetrahedron. The optimized molecular structure and the vibrational spectra were calculated by the density functional theory DFT methods and the semi-empirical PM3 calculations. Dielectric study of this compound has been measured in order to determine the electrical conductivity type giving rise to an activation energy of $\Delta E\sigma=0.17$ eV.

Keywords Supramolecular structure · Hybrid material · Dielectric properties · DFT calculations · Semi-empiricalPM3 calculation

✉ Mohamed Boujelbene
m_boujelbene2010@yahoo.fr

[1] Laboratoire Physico-Chimie de l'Etat Solide LR11 ES51, Faculté des Sciences de Sfax, Université de Sfax, Route de Soukra Km 3.5, BP 802, 3071 Sfax, Tunisia

[2] Institut Préparatoire aux Etudes d'Ingénieur de Gabès, Université de Gabès, Rue Omar ibn el Khattab, CP: 6072 Gabès, Tunisia

[3] Laboratoire de Chimie Inorganique, Facultédes Sciences de Sfax, Universitéde Sfax, BP 1171, 3000 Sfax, Tunisia

Introduction

Organic–inorganic hybrid materials, constructed from the simultaneous incorporation of inorganic and organic components in a material, cover a broad range of application areas such as electrical [1, 2] magnetic [3, 4], optical and nonlinear optical [5, 6] electroluminescence [7] and ions [8, 9]. In class I of hybrids, according to Sanchez, the interaction between the organic and inorganic parts only occurs with weak bonds such as hydrogen, van der Waals or ionics [10]. Thus, these compounds with the characteristic of having supramolecular structures have interesting properties, like ferroelectricity [11] or optical properties [12]. The incorporation of an organic molecule, especially an amine, usually protonated, as the organic part provided many kinds of materials. The templating role of protonated amines [13–15] makes them important for optical and dielectric applications [16, 17]. In most of these materials, the amino cations interact with the inorganic part by weak hydrogen bonds. The synthesized hybrid compounds using arsenic acid and the organic molecule with aromatic rings lead to the different dimensionalities of the supramolecular structure, mostly maintained through strong hydrogen bonds like ribbons [18], chains [19–21], two-dimensional network [22, 23] and three-dimensional network [24]. In this context, we are interested in mixed hybrid salts of arsenate combining aromatic amine. Heterocyclic aminotriazole 5-amino-3-methyl-1-phenyl-1H-1,2,4-triazole ($C_9H_{10}N_4$), with a conformation that can be described as a phenyl ring linked to the triazole ring with the presence of one aliphatic C atom, was employed. This form would allow the contribution of the aromaticity, i.e., delocalization of electrons from the amine molecule in the case of dielectric behavior. The synthetic reaction with such amine provided a supramolecular structure type with non-centrosymmetric crystalline symmetry [21]. In general, optimizing the dielectric properties of supramolecular hybrid materials depends on many factors including the crystalline symmetry, the influence of the inorganic coordination polyhedron and hyperpolarizability of organic molecules. In this study, we synthesis a supramolecular hybrid dihydrogen arsenate salt using 5-amino-3-methyl-1-phenyl-1H-1,2,4-triazole. The XRD analysis shows that the obtained compound crystallizes in monoclinic symmetry, space group $P2_1$ with the formula $(C_9H_{11}N_4)H_2AsO_4$. The crystal structure of the novel compound is described in detail, and the most important interaction in the crystal is approved with the Hirshfeld surface analysis. The theoretical characterizations are carried out by using density functional theory DFT and the semi-empirical PM3 methods. A dielectric study including electrical conductivity is also presented.

Experimental section

Materials

5-Amino-3-methyl-1-phenyl-1H-1,2,4-triazole ($C_9H_{10}N_4$) is synthesized in the Laboratory [25] and used as received; arsenic acid (H_3AsO_4) is acquired from commercial sources and used as received.

Chemical preparation

The compound $(C_9H_{11}N_4)H_2AsO_4$ is obtained by slow evaporation at room temperature. 5-Amino-3-methyl-1-phenyl-1H-1,2,4-triazole is dissolved in 10 ml of water and arsenic acid with the appropriate molar ratio 1:1. The clear solution is stirred until the complete dissolution and is allowed to stand at room temperature. Single transparent colorless parallelepiped crystals appeared after a few days. Then, the products were filtered off and washed with a small amount of distilled water.

Reaction scheme:

$$C_9H_{10}N_4 + H_3AsO_4 \xrightarrow{H_2O} \left(C_9H_{11}N_4\right)^+\left(H_2AsO_4\right)^-$$

Infrared spectroscopy

Spectrum was recorded in the wavenumber range of 4000–500 cm^{-1} with a "Perkin–Elmer FTIR" spectrophotometer 1000 using a dispersed sample in spectroscopically pure KBr pellet.

X-ray data collection and structure determination

A suitable crystal of the compound was glued to a glass fiber mounted on a Bruker APEX-II Kappa CCD diffractometer. Intensity data sets were collected using AgK radiation ($\lambda = 0.56087$ Å) at 293 K. The crystal structure of $(C_9H_{11}N_4)H_2AsO_4$ was solved in the monoclinic symmetry space group $P2_1$. The structure was solved with a direct method from the SHELXS-97 programs [26], which permitted the identification of the location of the AsO_4 group. The remaining non-hydrogen atoms were located by successive difference Fourier maps using the SHELXL-97 programs [27]. The hydrogen atoms were fixed geometrically by the appropriate instructions of the SHELXL-97 programs. The figures of the structural part were performed with Diamonds software [28]. The crystal data and structure solution and refinement information are listed in Table 1.

Hirshfeld surfaces calculations

Hirshfeld surface analysis [29–36] is performed with CrystalExplorer (Version 3.1) [37] to further understand the relative contributions of intermolecular interactions

Table 1 Crystal data and structure refinement details of $(C_9H_{11}N_4)H_2AsO_4$

Formula/formula weight	$C_9H_{11}AsN_4O_4$/314.031 $gmol^{-1}$
Crystal system	Monolinic
Space group/*Z*	$P2_1/2$
Lattice parameters	$a = 9.655$ (3) Å; $b = 4.7090$ (15) Å; $c = 14.022$ (4) Å
Volume $Å^3$	605.8 (3)
Density (calculated) (g/cm^3)	1.722
Absorption coefficient (mm^{-1})	2.82
F(0 0 0)	316
Wavelength, Mo	$K\alpha = 0.71073$ Å
Temperature	100 K
Theta range	1.5°/28.1°
h, *k*, *l* range	− 12/12, − 6/5, − 16/18
No. of independent reflections	2501
Unique reflections included: ($I > 2\sigma I$)	2389
No. of refined parameters	176
R	0.032
Rw	0.089
$Dr_{min}./Dr_{max}.$ ($e/Å^3$)	− 0.79/0.88
CCDC number	2181160

by various molecular contacts in the crystal packing of the synthesized hybrid compound $(C_9H_{11}N_4)H_2AsO_4$.

Impedance analysis

The electrical impedances were measured in the range between 1 kHz and 13 MHz using a Hewlett-Packard 4192A LF automatic bridge interfaced to compatible HP Vectra microcomputer. Moreover, complex impedance measurements were performed using a compressed pellet of 5 mm diameter. Metallic silver was deposited on both sides of served electrodes. The electrical properties were collected under stagnant air atmosphere and determined by impedance and modulus method using a frequency response analyzer.

Theoretical calculation method

Density functional theory DFT and semi-empirical PM3 calculations methods were performed using the GAMESS series of programs [38] without any symmetry restrictions (Figs. S1 and S2). We have tested the B3LYP functional in reproducing the observed values of the vibrational frequencies of $(C_9H_{11}N_4)H_2AsO_4$. In our study, there is a spectral overlap between the vibration areas of organic and inorganic ions. Therefore, owing to the difficulty of precise allocation of the observed

IR bands, we resorted to calculations ab initio, density functional theory and semi-empirical, so as to determine harmonic frequencies of vibration modes. The calculated frequencies are corrected by a scale factor "*F*." The factor *F* is determined after the frequency comparison calculated with the method ab initio (MP2//accpvdz) and the PM3 method of the anion $[H_2AsO_4]^-$ (*F* value = MP2/value PM3). The results reported in Table S1 show that the *F* factor is more than 1 for stretching modes and lower than 1 for the deformation modes. Therefore, we adopted two *F* values (F_1 and F_2). F_1 is the average value of the scaled factors for stretching modes ($F_1 = 0.93$) and F_2 corresponding to the scaled factors for deformation modes ($F_2 = 1.14$). We performed calculations of density functional theory DFT with a aug-ccpVDZ base and the semi-empirical method PM3, taking into account the effect of intermolecular interactions on geometrical parameters. We have considered that the compound built up from one $[H_2AsO_4]^-$ anion and one $C_9H_{11}N_4$ cation linked by N–H…O et O–H···O hydrogen bonds. All observed vibrational bands have been discussed and assigned to normal mode or to combinations on the basis of our density functional theory DFT and semi-empirical PM3 calculations in Table 2. To identify the calculated modes, we used the Molden [39] graphical package.

Results and discussion

Structural crystallography

Hybrid dihydrogen arsenate salt with formula $(C_9H_{11}N_4)H_2AsO_4$ crystallizes in the monoclinic symmetry, with the non-centrosymmetric space group$P2_1$. The asymmetric unit of the supramolecular structure (Fig. 1) is formed by one organic monoprotonated amine $[C_9H_{11}N_4]^+$ and one inorganic anion $[H_2AsO_4]^-$. In the crystal packing, anionic inorganic dimers are formed by two adjacent dihydrogen arsenate tetrahedron $[H_2AsO_4]^-$ interconnected by O–H···O hydrogen bonds ranging between 1.710 and 1.760 Å, while the organic molecules are bonded to these mineral dimers entities through N–H···O hydrogen bonds ranging between 1.799 Å and 2.129 Å. The association of organic and inorganic parts gives rise to a crystal structure with a fully supramolecular network. The inorganic and organic parts alternate along the crystallographic c axis (Fig. 2). Protonated amine molecules are incorporated parallel to (a, b) plane, to ensure electroneutrality with mineral dimers of anions. Within the $[H_2AsO_4]^-$ tetrahedra, the distance of the two As–OH bonds (1.701 and 1.715 Å) is significantly longer than of the other two As–O bonds (1.660 and 1.672 Å) depending on the nature of the oxygen atom. Within the organic amine molecule, the C–N, C–C and C = S distances are close to the usual values observed in others homologous derivatives.

Hirshfeld surface analysis

Hirshfeld surface analysis is performed to further explain intermolecular interactions in the crystal packing. The results, shown in Fig. 3, revealed that in all possible

Table 2 Experimental and calculated infrared vibration wavenumbers (cm^{-1}) of $(C_9H_{11}N_4)H_2AsO_4$ with proposed assignments

Experimental	Calculated Semi-empiric	Calculated DFT	Attribution
3267	3356	3223	ν(OH(
2980	2941	2994	ν_s(C–H) met + ν_s(N_4–H)
2970	2863	2864	ν_{as} (C–H)met + ν_s(C–H)$_{ar}$
2907	2902	2860	ν_{as} (N_4–H)
2745	2847	2757	ν_{as}(C–H)$_{ar}$
	2842	2744	
	2840		
2697	2564	2733	ν(N_3–H)
1816	1822	1806	δ(NH_2)
1655	1653	1651	ν(C = C)
	1646		
1597	1579	1599	(CH_3)
	1573	1590	
1591	1635	1651	ν(C–N)
1502	1560	1535	ν(C–NH_2)
1451	1451	1442	δ(NH)
1398	1385	1388	ν(C–C–N)
	1341	1376	
1325	1228	1324	δ(C–H)$_{ar}$
1225	1236	1246	ν(C–N) + ν(C–C)
	1221	1229	
1092	1069	1064	γ(C–H)ar
1030	991	1027	δ(NH_2)
1002	959	992	γ(CH)ar
919	850	855	
864	895	890	γ(CH)$_{ar}$ + δ(NH_2)
	820	818	δ(N_3–H) + δ(OH)
792	818	814	ν_3(AsO_4)
755	760	751	υ1(AsO_4)
696	712	687	δ(CCC)$_{ar}$
684	646	678	γ(CCC)$_{ar}$
651	612	650	
574	557	579	
629	518	620	ν_4(AsO_4)

ν (stretching); δ (in plane bending); γ (out of plane bending); ar (aromatic ring); met (methyl group)

molecular contacts, hydrogen–hydrogen contacts predominate, contributing 37.5% of the overall intermolecular interactions. The second most significant intermolecular interaction is oxygen–hydrogen, resulting in 31.9% of the sum of intermolecular interactions. In addition, H···C and H···N interactions also contribute to the total

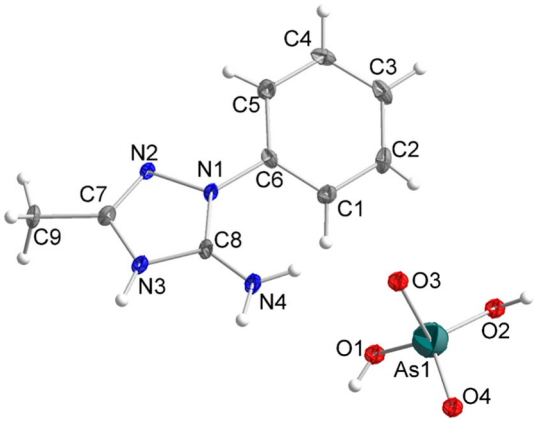

Fig. 1 Asymmetric unit representation of $(C_9H_{11}N_4)H_2AsO_4$

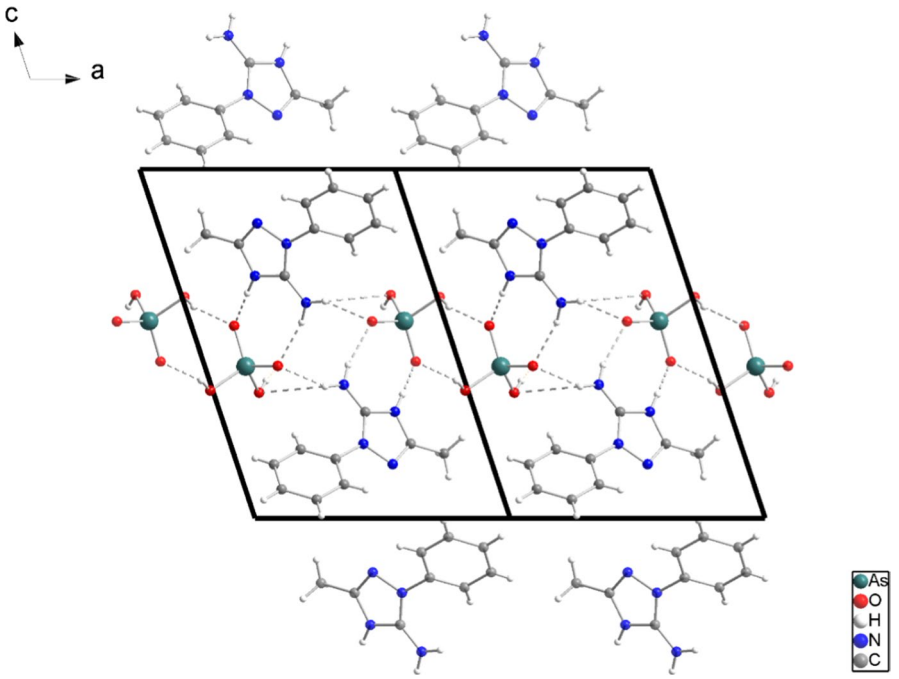

Fig. 2 Projection of the structure of $(C_9H_{11}N_4)H_2AsO_4$ along the crystallographic *b* axis, showing its supramolecular aspect

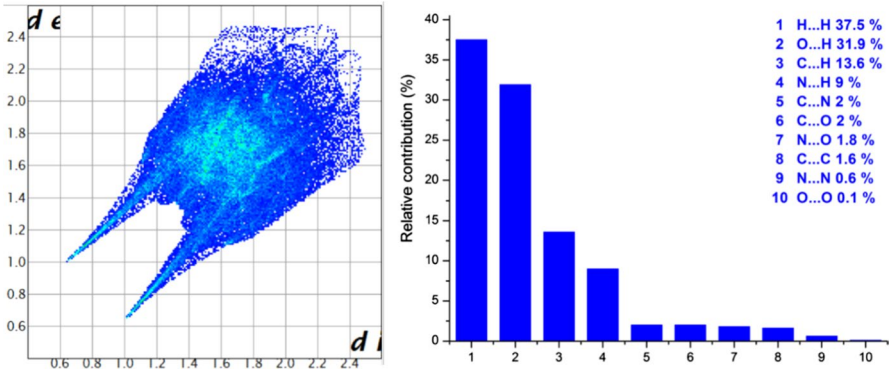

Fig. 3 Fingerprint plots and percentage contributions of the various intermolecular contacts contributing to the Hirshfeld surfaces of $(C_9H_{11}N_4)H_2AsO_4$

intermolecular interactions with 13.6% and 9%, respectively. In general, the crystalline structure is stabilized by different interactions.

Vibrational analysis

For visual comparison, the observed and simulated IR spectra are presented in Fig. 4. All observed vibrational bands have been discussed and assigned to normal mode or to combinations on the basis of density functional theory DFT and semi-empirical PM3 calculations (Table 2) as a primary source of attribution and also by comparison with the previous results for similar compound [40]. The arsenate ion in solution is known to have tetrahedral symmetry, its molecular group being Td [41, 42]. Its four fundamental bands have the following frequencies: $\upsilon_3(F_2) = 805$, $\upsilon_1(A_1) = 775$, $\upsilon_4(F_2) = 396$ and $\upsilon_2(E) = 335$ cm^{-1}. Due to the lowering of the symmetry from an ideal configuration and the crystal field effect, the splitting can be observed for the doubly degenerated υ_2 mode for, the triply degenerated υ_3 and υ_4 modes. Bands derived from internal vibrations of arsenate anions were detected, and their assignment is given in Table 2. The ν_1 mode is observed as a strong peak at 755 cm^{-1} in the IR observed spectrum and appears at 751 cm^{-1} and 760 cm^{-1} from DFT and MP3 calculations, respectively. The medium band which that occurs at 792 cm^{-1} is characteristic for ν_3 (AsO_4), while the theoretically computed values by the DFT method appears at 814 cm^{-1} and by semi-empirical PM3 method appears at 818 cm^{-1}. These values are similar to those observed in the structure of $C_3H_9AsN_6O_4$ [43]. The stretching vibration of C = C is observed at 1655 cm^{-1} from the IR spectrum in accordance with the semi-empirical PM3 calculations detected at 1653 and 1646 cm^{-1}, and with DFT calculations detected at 1651 cm^{-1}. The C–N bond asymmetric stretching vibration is observed in the IR spectrum at 1591 and 1225 cm^{-1} and is evidenced by calculated values with density functional theory DFT at 1651 and 1246 cm^{-1} and calculated values by the semi-empirical method MP3 at 1635 and 1236 cm^{-1}. The IR observed spectrum reveals also a broad and strong band

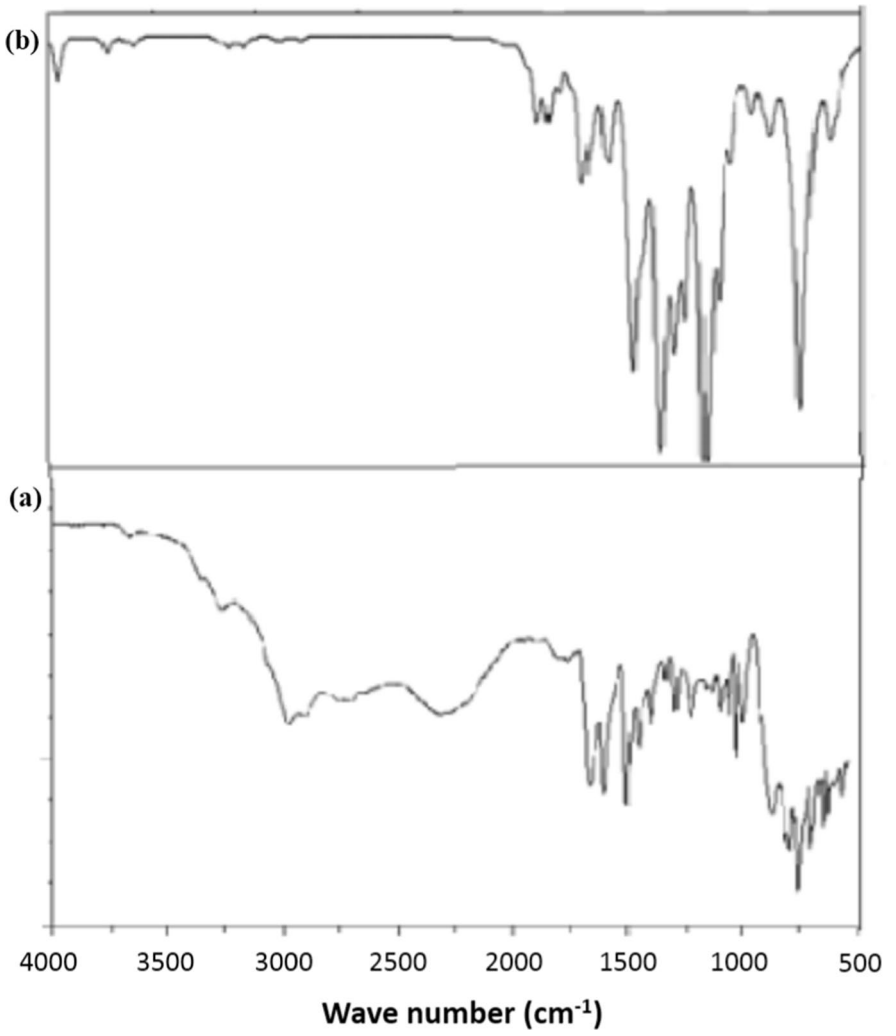

Fig. 4 Experimental (**a**) and calculated (**b**) infrared spectra of $(C_9H_{11}N_4)H_2AsO_4$ recorded at room temperature in the range of 4000–500 cm^{-1}

at 3660 cm^{-1}, which may be assigned to the stretching mode ν (OH). The theoretically computed identified this assignment at 3223 cm^{-1} and at 3356 cm^{-1} by the DFT method and semi-empirical PM3 method, respectively. The asymmetric stretching modes corresponding to $(C–H)_{ar}$ are observed from bands located at 2980, 2970 and2745 cm^{-1} in observed IR spectra. These values are calculated at 2994, 2864 and 2757 cm^{-1} by the density functional theory DFT method, and at 2941, 2863 and 2847 cm^{-1} from the semi-empirical method MP3.

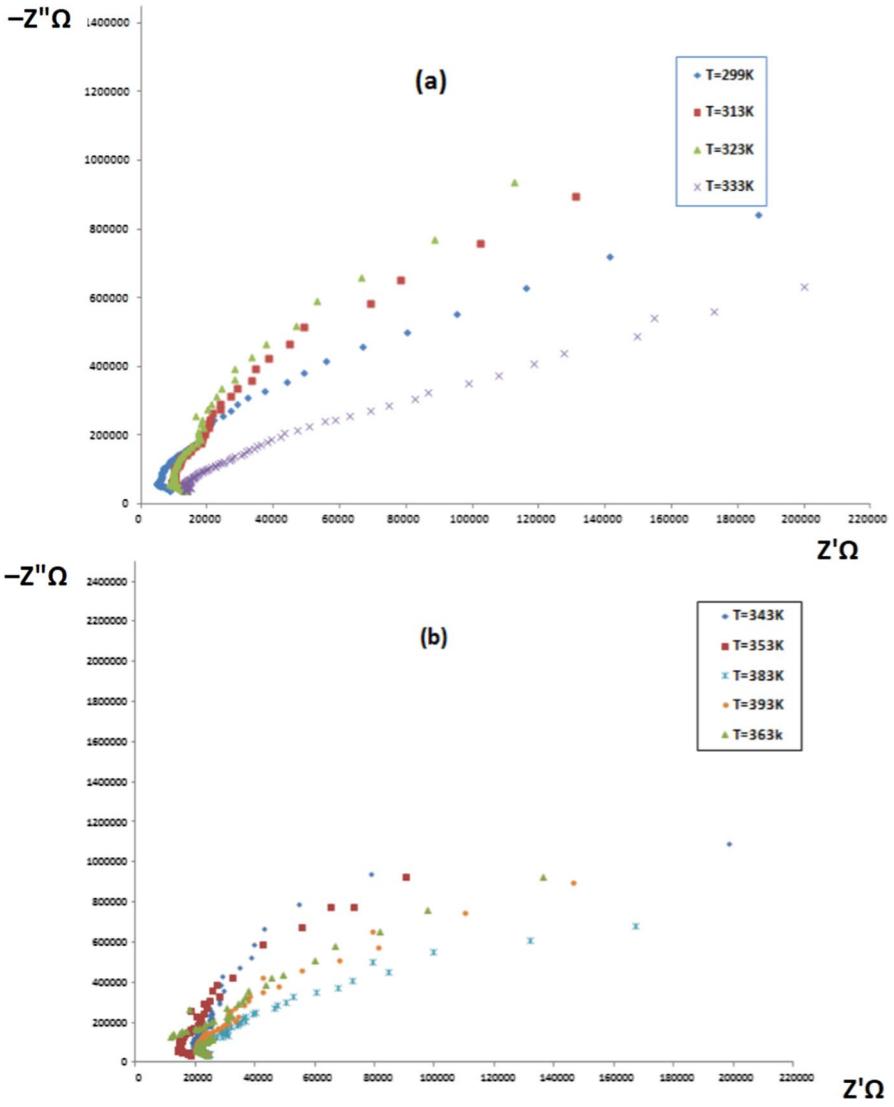

Fig. 5 Complex impedance diagrams $-Z''$ versus Z' for $(C_9H_{11}N_4)H_2AsO_4$ from 299 to 333 K (**a**) and from 343 to 363 K (**b**)

Electrical conductivity

Typical impedance spectra were obtained at different temperatures ranging from 299 to 408 K for $(C_9H_{11}N_4)H_2AsO_4$ (Fig. 5a, b). The bulk ohmic resistance relative to each experimental temperature is the intercept on the real axis of the zero-phase angle extrapolation of the highest-frequency curve. The resistance was determined by extrapolation of the circular arc centered under the Z_0 axis to zero frequency which defines an

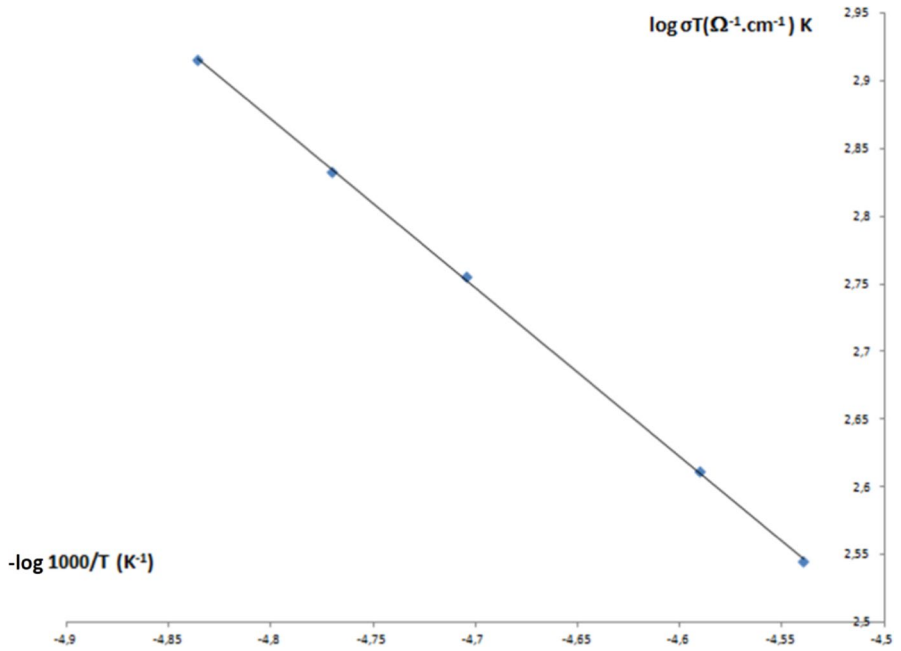

Fig. 6 Temperature dependences of $\log(\sigma T) = f(-\log 10^3/T)$ for $(C_9H_{11}N_4)H_2AsO_4$

[$\alpha(\pi/2)$] dispersion angle ($\alpha = 0.3$) [44]. This shows that $(C_9H_{11}N_4)$ (H_2AsO_4) follows the Cole–Cole law.

$\varepsilon^* = \varepsilon_\infty + (\varepsilon_\infty - \varepsilon_s)/(1 + (j\omega\tau)^{1-\alpha})$ where ε^* is the complex dielectric constant, ε_s and ε_∞ are the "static" and "infinite frequency" dielectric constants, ω is the angular frequency and τ is a time constant. The coefficient at which characterizes the deviation of the Cole–Cole from the Debye law.

$\varepsilon = \varepsilon_\infty + (\varepsilon_\infty - \varepsilon_s)/(1 + j\omega\tau)$ is determined from the complex impedance spectrum. These curves show the temperature dependence of the resistance proving the high conductivity properties of $[C_9H_{11}N_4]$ $[H_2AsO_4]$.

Figure 6 shows the temperature dependence of the conductivity in a log (σT) versus –log1000/T indicating an Arrhenius type behavior. In order to understand the conduction phenomenon, we used the Arrhenius modeling equation: $\sigma(T) = A \exp(-E_a/k_bT)$, where E_a is the activation energy, σ is the conductivity (obtained from R by means of the relation: $\sigma = e/RS$, where e/S represents the geometrical ratio sample), A is the pre-exponential factor, k_b is the Boltzmann constant, and T is the temperature [45]. The conductivity plot, in this region, exhibits one part. The activation energy is of $\Delta E\sigma = 0.17$ eV.

Conclusion

The present research work reported the synthesis and the crystal structure determination of a new hybrid dihydrogen arsenate material that combines the organic amine molecule 5-amino-3-methyl-1-phenyl-1H-1,2,4-triazole, with the formula $(C_9H_{11}N_4)H_2AsO_4$. The crystallographic study showed that this compound crystallizes in the non-centrosymmetric monoclinic system, space group $P2_1$. The supramolecular structural feature built from isolated inorganic anionic entities and organic cationic molecules are linked together with hydrogen bonds and weak interactions only. A good correlation is found between the theoretical calculation (density functional theory DFT and semi-empirical PM3 methods) and the experimental results. The dielectric measurement according to the temperature has demonstrated that the conductivity measurement follows the Arrhenius approach and the activation energy is $\Delta E\sigma = 0.17$ eV.

Supplementary Information The online version contains supplementary material available at https://doi.org/10.1007/s00289-023-04670-3.

Acknowledgements Funding was provided by 12 (Grant No. 3).

Declarations

Conflict of interest Hybrid dihydrogen arsenate salt with formula $(C_9H_{11}N_4)H_2AsO_4$ crystallizes in the monoclinic symmetry, with the non-centrosymmetric space group $P2_1$. The asymmetric unit of the supramolecular structure is formed by one organic monoprotonated amine $[C_9H_{11}N_4]^+$ and one inorganic anion $[H_2AsO_4]^-$. In the crystal packing, anionic inorganic dimers are formed by two adjacent dihydrogen arsenate tetrahedron $[H_2AsO_4]^-$ interconnected by O–H···O hydrogen bonds ranging between 1.710 and 1.760 Å, while the organic molecules are bonded to these mineral dimers entities through N–H···O hydrogen bonds ranging between 1.799 and 2.129 Å. The association of organic and inorganic parts gives rise to a crystal structure with a fully supramolecular network. The inorganic and organic parts alternate along the crystallographic c axis.

References

1. Teophil E, Siegfried H (2003) The chemistry of heterocycles: structures, reactions, synthesis, and applications. Wiley, New York, p 422
2. Zhou HX (2010) Piperazine-1,4-diium bis(2-carboxy-1H-pyrazole-4-carboxylate) tetrahydrate. Acta Cryst E 66:2578
3. Manteghi F, Ghadermazi M, Kakaei N (2011) Piperazine-1,4-diium pyridine-2,3-dicarboxylate methanol monosolvate. Acta Cryst E 67:1122

4. Peng C (2010) Piperazine-1,4-diium bis(perchlorate) dehydrate. Acta Cryst E 66:2214
5. Polishchuk VA, Karaseva TE, Pushilin AM (2009) Piperazine-1, 4 diium bis [tetrachloridoaurate(III)] dihydrate. Acta Cryst E 65:m1377
6. Wang L, Zheng H, Jia L (2008) Three-dimensional network in piperazine-1,4-diium-picrate-piperazine (1/2/1). Acta Cryst E 64:665
7. Usman A, Chantrapromma S, Fun KH, Poh LB, Karalai C (2002) Phase transitions in hydrogen-bonded phenol-amine adducts: analysis by ferroelastic theory. Acta Cryst C 58:136
8. Hu Y, Peng C, Li P (2010) R)-2-Methylpiperazine-1,4-diium diaquatetrachloridoferrate(II). Acta Cryst E 66:m1224
9. Kefi R, Lefebvre F, Zeller M, Ben C (2011) Nasr 1-(2,5-Dimethylphenyl)piperazine-1,4-diium tetrachloridozincate monohydrate. Acta Cryst E 67:m410
10. Sanchez C, Ribot F (1994) Design of hybrid organic–inorganic materials synthesized via sol–gel chemistry. New J Chem 18:1007
11. Kirpichnikova LF, Shuvalov LA, Ivanov NR (1989) Ferroelectricity in the dimethylaminaluminium-sulphate crystal. Ferroelectrics 96:313–317
12. Ushasree PM, Jayavel R, Subramanian C, Ramasamy P (1999) Growth of zinc thiourea sulfate (ZTS) single crystals: a potential semiorganic NLO material. J Cryst Growth 197:216
13. Gerardin C, Loiseau T, Ferey G, Taulelle F, Navrotsky A (2002) Thermochemistry of amine-templated open frameworks. A Chem Mater 14:3181
14. Yao H-B, Gao M-R, Yu SH (2010) Small organic molecule templating synthesis of organic–inorganic hybrid materials: their nanostructures and properties. Nanoscale 2:323
15. Rao CNR, Natarajan S, Choudhury A, Neeraj S, Ayi AA (2001) Aufbau principle of complex open-framework structures of metal phosphates with different dimensionalities. Acc Chem Res 34:80
16. Leblanc N, Allain M, Mercier N, Sanguinet L (2011) Stable photoinduced separated charge state in viologen halometallates: some key parameters. Cryst Growth Des 11:2064
17. Bi W, Louvain N, Mercier N, Luc J, Rau I, Kajzar F, Sahraoui B (2008) A switchable NLO organic–inorganic compound based on conformationally chiral disulfide molecules and $Bi(III)I_5$ iodobismuthate networks. Adv Mater 20:1013
18. Baouab L, Jouini A (1998) Crystal structures and thermal behavior of two new organic monophosphates. J Solid State Chem 41:343
19. Averbuch-Pouchot MT, Durif A (1987) Structures of ethylenediammonium monohydrogen tetraoxophosphate(V) and ethylenediammonium monohydrogentetraoxoarsenate(V). Acta Cryst C 43:1894
20. Averbuch-Pouchot MT, Durif A, Guitel JC (1988) Structures of β-alanine, DL-alanine and sarcosine monophosphates. Acta Cryst C44:1968
21. Chtourou A, Boujelbene M, Allouch F, Mhiri T (2014) Synthesis, crystal structure and characterization of $[C_9H_{11}N_4]$ H_2PO_4. Mol Struct 1063:153
22. Averbuch-Pouchot MT, Durif A, Guitel JC (1988) Structures of glycine monophosphate and glycine *cyclo*-triphosphate. Acta Cryst C C 44:99
23. Bagieu-Beucher M (1990) Structure of cytosinium dihydrogenmonophosphate. Acta Cryst C465:238
24. Bagieu-Beucher M, Durif A, Guitel JC (1989) Structure of ethylenediammonium dihydrogentetraoxophosphate(V) pentahydrogenbis[tetraoxophosphate(V)]. C Acta Cryst 45:421
25. Allouch F, Zouari F, Chabchoub F, Salem M (2008) 5-Amino-3-methyl-1-phenyl-1*H*-1,2,4-triazole. Acta Cryst E 64:684
26. Guerfel T, Jouini A (2001) Crystal structure, thermal analysis, and IR spectrometric investigation of 1,2-diammonium-2-methyl propane sulfate monohydrate. J Chem Cryst 31:333
27. Baur WH (1974) The geometry of polyhedral distortions. Predictive relationships for the phosphate group. J Acta Cryst B 30:1195
28. Brandenburg K (1998) Diamond version 2.0 Impact GbR, Bonn, Germany
29. Mckinnon JJ, Mitchell AS, Spackman MA (1998) Hirshfeld surfaces: a new tool for visualising and exploring molecular crystals. Chem Eur J 4:2136
30. Spackman MA, Byrom PG (1997) A novel definition of a molecule in a crystal. Chem Phys Lett 267:215
31. McKinnon JJ, Jayatilaka D, Spackman MA (2007) Towards quantitative analysis of intermolecular interactions with Hirshfeld surfaces. Chem Commun 66:3814
32. Spackman MA, Jayatilaka D (2009) Hirshfeld surface analysis. CrystEng Comm 11:19

33. Bitzer RS, Visentin LC, Horner M, Nascimento MAC, Filgueiras CAL (2017) On the molecular and supramolecular properties of *N*,*N*′-disubstituted iminoisoindolines: synthesis, spectroscopy, X-ray structure and Hirshfeld surface analyses, and DFT calculations of two (E)-N,N′-bis(aryl)iminoisoindolines (aryl = *2-te*rt-butylphenyl or perfluorophenyl). J Mol Struct 1130:165
34. Madura ID, Zachara J, Hajmowicz H, Synoradzki L (2012) Interplay of carbonyl–carbonyl, C-H···O and C–H···π interactions in hierarchical supramolecular assembly of tartaric anhydrides—tartaric acid and its *O*-acyl derivatives: part 11. J Mol Struct 1017:98
35. Spackman MA, Mckinnon JJ (2002) Fingerprinting intermolecular interactions in molecular crystals. CrystEng Comm 4:378
36. Koenderink JJ, Van Doorn AJ (1992) Surface shape and curvature scales. Image Vis Comput 10:557
37. Wolff SK, Grimwood DJ, Mckinnon JJ, Turner MJ, Jayatilaka D, Spackman MA (2010) Crystal Explorer 3.1. University of Western Australia
38. Schmidt MW, Baldridge KK, Boatz JA, Elbert ST, Gorden MS, Jensen JH, Koseki S, Matsunaga N, Nguyen KA, Su SJ, Windus TL, Dupuis M, Montgomery JA (1993) General atomic and molecular electronic structure system. J Comput Chem 14:1347
39. Schaftenaar G, Noordik JH (2000) Molden: a pre- and post-processing program for molecular and electronic structures. J Comput Aided Mol Des 14:123
40. Ahmeda AB, Feki H, Abid Y, Minot C (2010) Molecular structure, vibrational spectra and nonlinear optical properties of orthoarsenic acid-tris-(hydroxymethyl)-aminomethane DFT study. Spectrochimica Acta Part A 1315:75
41. Herzberg G (1945) Molecular spectra and molecular structure, vol II. Van Nostrand, New York
42. Nakamoto K (1963) Infrared spectra of inorganic and coordination compounds. Wiley, New York
43. Anbalagan G, Marchewka MK, Pawlus K, Kanagathara N (2015) Crystal structure and vibrational spectra of melaminium arsenate. J Mol Struct 1079:407
44. Hassen CB, Boujelbene M, Bahri M, Zouari N, Mhiri T (2014) Experimental study on the structure and vibrational, thermal and dielectric properties of bis(2-methylanilinium) selenate accomplished with DFT calculation. J Mol Struct 1074:602
45. Bauerle JF (1969) Study of solid electrolyte polarization by a complex admittance method. J Chem Phys 30:2657